



AMS and LC/MS analyses of SOA from the photooxidation of benzene and 1,3,5-trimethylbenzene in the presence of NO_x: effects of chemical structure on SOA aging

K. Sato¹, A. Takami¹, Y. Kato^{1,*}, T. Seta¹, Y. Fujitani¹, T. Hikida², A. Shimono², and T. Imamura¹

¹National Institute for Environmental Studies, 16-2 Onogawa, Tsukuba, Ibaraki 305-8506, Japan

²Shoreline Science Research Inc., 3-12-7, Owada-machi, Hachioji, Tokyo 192-0045, Japan

* currently at: Nuclear Material Control Center, 1-28-9 Higashi-Ueno, Taito, Tokyo 110-0015, Japan

Correspondence to: K. Sato (kei@nies.go.jp)

Received: 19 December 2011 – Published in Atmos. Chem. Phys. Discuss.: 3 January 2012

Revised: 10 May 2012 – Accepted: 10 May 2012 – Published: 25 May 2012

Abstract. Oxygenated organic aerosol (OOA) observed in remote areas is believed to comprise aged secondary organic aerosol (SOA); however, the reaction processes relevant to SOA chemical aging have hitherto been unclear. We recently measured the mass spectra of SOA formed from the photooxidation of aromatic hydrocarbons using an Aerodyne aerosol mass spectrometer (AMS) and reported that SOA aging is slowed with increasing number of alkyl groups in the precursor molecule. In this study, we selected benzene and 1,3,5-trimethylbenzene (TMB) as precursors to analyze SOA formed from the photooxidation of aromatic hydrocarbons in the presence of NO_x using high-resolution time-of-flight AMS (H-ToF-AMS) and liquid chromatography/time-of-flight mass spectrometry (LC/TOF-MS). A van Krevelen diagram was studied using the O/C and H/C ratios obtained by H-ToF-AMS for organics present in SOA. The results showed these organics to be rich in carboxylic acids or hydroxycarbonyls and the O/C ratio of SOA formed by the reaction of 1,3,5-TMB to be lower than that for benzene. Analytical results from LC/TOF-MS showed the particulate products formed by the reaction of 1,3,5-TMB to be richer in ketocarboxylic acids than for benzene. These results indicate that SOA aging proceeds mainly by formation of carboxylic acids and that the rate of SOA aging in laboratory chambers is limited by the oxidation of ketone groups. SOA formed in laboratory chamber experiments is less oxidized than for ambient OOA, not only because the experimental duration is insufficient or the SOA mass loading in the chamber is higher than that of the atmosphere. The laboratory chamber

experiments under dry conditions are not able to simulate ketocarboxylic acid photochemical oxidation in the aqueous phase. The fractions of organic peroxides to the total SOA mass were determined by iodometric spectrophotometry to be $12 \pm 8\%$ (1,3,5-TMB) and $<39\%$ (benzene). Further, it was newly found that, unlike the reaction of benzene, only very small amounts of nitrophenols are produced by the reaction of 1,3,5-TMB.

1 Introduction

Atmospheric organic aerosol is believed to affect human health, climate, and visibility (Kroll and Seinfeld, 2008; Hallquist et al., 2009). Field observations using an Aerodyne aerosol mass spectrometer (AMS) have revealed the organic aerosol observed in remote areas to be rich in oxygenated organic aerosol (OOA) (Zhang et al., 2007; Takami et al., 2007; Lun et al., 2009; Takegawa et al., 2009). Since secondary organic aerosol (SOA) formed in laboratory chamber experiments is less oxidized than ambient OOA, ambient OOA is assumed to be aged SOA (Bahreini et al., 2005; Alfara et al., 2006; Chhabra et al., 2010, 2011). To understand the formation process of atmospheric OOA, the aging process of SOA is currently a focus of research interest in the field of atmospheric chemistry (Kroll and Seinfeld, 2008; Qi et al., 2010; Chen et al., 2011; Shiraiwa et al., 2011; Lambe et al., 2011; Loza et al., 2012).

Table 1. Experimental conditions and SOA yields.

| Run number | Hydrocarbon (HC) | [HC] ₀ (ppb) | [NO _x] ₀ (ppb) ^a | [CH ₃ ONO] ₀ (ppb) ^b | ΔHC (μg m ⁻³) ^c | SOA mass conc. (μg m ⁻³) ^d | SOA Yield (%) ^{e,f} |
|------------|------------------|-------------------------|--|---|--|---|------------------------------|
| Run 1 | benzene | 1834 | 102 | 2 | 1070 | 18 | 1.8 ± 0.2 |
| Run 2 | benzene | 1466 | 889 | 1093 | 608 | 49 | 8.0 ± 1.4 |
| Run 3 | benzene | 4163 | 999 | 1078 | 635 | 198 | 31.2 ± 10.7 |
| Run 4 | 1,3,5-TMB | 1002 | 200 | 2 | 2242 | 54 | 2.5 ± 0.1 |
| Run 5 | 1,3,5-TMB | 1455 | 974 | 50 | 4522 | 160 | 3.7 ± 0.2 |
| Run 6 | 1,3,5-TMB | 1515 | 1052 | 1036 | 5913 | 920 | 15.6 ± 1.0 |

^a NO₂/NO ratio was ~0 (Runs 1 and 4, low mass loading experiments) or ~3 (Runs 2, 3, 5, and 6, high mass loading experiments), ^b Used as OH radical source, ^c Hydrocarbon reacted, ^d SOA mass concentrations were calculated using SMPS volume concentrations and a density of 1.4 g cm⁻³; no correction of SOA wall loss deposition was carried out, ^e SOA yield was determined dividing the mass concentration of aerosol produced by the concentration of hydrocarbon reacted (errors are 2σ), ^f Using the rate of particle wall deposition loss (3 × 10⁻⁵ s⁻¹, Sato, 2008), the SOA yields listed are corrected to 2.2 % (Run 1), 8.3 % (Run 2), 32.0 % (Run 3), 2.9 % (Run 4), 4.1 % (Run 5), and 16.5 % (Run 6).

If the chemical composition changes as SOA ages, the physical and chemical properties of aerosol particles such as the volatility, hygroscopicity, toxicity, and the optical properties will also change (e.g., Jimenez et al., 2009; Kroll and Seinfeld, 2008; Wang et al., 2012; Zhang et al., 2011). Concerning its toxicity and optical properties, specific molecules will strongly influence the overall property of OOA particles. For example, quinones and organic peroxides present in SOA are known to induce oxidative stress (Baltensperger et al., 2008; Wang et al., 2011); and nitrophenols, which are also present in SOA, show optical absorption in the visible region (Nakayama et al., 2010; Zhang et al., 2011). Understanding of SOA aging at the molecular level is necessary for better understanding of the impact of OOA.

Aromatic hydrocarbons are typical SOA precursors emitted into the atmosphere from anthropogenic emission sources (Calvert et al., 2002; Henze et al., 2008; Lane et al., 2008). The SOA yield (Izumi and Fukuyama, 1990; Odum et al., 1997; Hurley et al., 2001; Takekawa et al., 2003; Sato et al., 2004; Song et al., 2005; Martin-Reviejo and Wirtz, 2005; Ng et al., 2007), the SOA chemical composition (Forstner et al., 1997; Jang and Kamens, 2001; Kalberer et al., 2004; Fisseha et al., 2004; Hamilton et al., 2005; Irei et al., 2006, 2011; Sato et al., 2007, 2010; Huang et al., 2007; Borrás and Tortajada-Genaro, 2012), and the reaction mechanism relevant to SOA formation (Stroud et al., 2004; Johnson et al., 2004, 2005; Bloss et al., 2005; Hu et al., 2007; Kelly et al., 2010) have been a focus of research into the atmospheric oxidation of aromatic hydrocarbons.

We recently measured SOA formed from the photooxidation of aromatic hydrocarbons using AMS and reported that SOA aging is slowed by increasing the number of alkyl groups in the precursor aromatic molecule (Sato et al., 2010). Very recently, a triangle plot technique for analysis of organic aerosol aging (Ng et al., 2010) and new numerical or graphical analysis methods using the elemental analysis data obtained by high-resolution time-of-flight AMS (H-ToF-AMS)

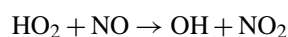
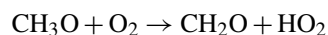
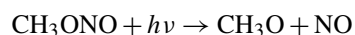
(Chhabra et al., 2010, 2011; Kroll et al., 2011; Ng et al., 2011) have been developed.

In this study, we selected benzene and 1,3,5-trimethylbenzene (TMB) as SOA precursors for analysis of SOA formed in photooxidation chamber experiments in the presence of NO_x (NO and NO₂) using H-ToF-AMS and liquid chromatography/time-of-flight mass spectrometry (LC/TOF-MS). New presentation methods of AMS data employing the van Krevelen diagram or triangle plot were used to obtain a better understanding of the relationship between the chemical structure of the reactant and SOA aging. LC/TOF-MS analysis yielded molecular-level information. The aims of this study were to elucidate the major reaction processes relevant to SOA aging and to study possible factors that limit the rate of SOA aging.

2 Experimental section

2.1 Experimental procedure

The details of the experimental procedure are explained elsewhere (Sato et al., 2004, 2007, 2010). All experiments were conducted using a 6-m³, evacuable, Teflon-coated stainless steel chamber (Akimoto et al., 1979). Hydrocarbons, NO_x, methyl nitrite, and purified air were mixed in the chamber (Table 1). Methyl nitrite was added as the OH radical source:



Methyl nitrite was prepared by dropping 50 % w/w aqueous sulfuric acid onto methanolic sodium nitrite and was used after vacuum distillation to remove any methanol and NO_x impurities. No NO_x impurity was detected by an FT-IR spectrometer with an optical length of 221.5 m (Thermo-Fisher Nexus 670, 1 cm⁻¹ resolution, NO detection limit = 7.9 ppb, NO₂ detection limit = 0.95 ppb) when 1 ppm methyl nitrite

was introduced in the chamber. The temperature of the gaseous mixture was maintained at 298 ± 1 K. The relative humidity of the purified air was ~ 0.003 %. No seed particles were added. The gaseous mixture was irradiated by light from 19 Xe arc lamps (1 kW each) through Pyrex filters for 4–11 h. The rate constant of the NO₂ photolysis was 0.29 min^{-1} .

Hydrocarbon, methyl nitrite, NO, NO₂, and O₃ were monitored using FT-IR spectrometer. The size distribution of particles was measured using a scanning mobility particle sizer (SMPS, TSI, model 3934) to calculate the volume concentration. The chemical composition of the particles was analyzed using an AMS (Aerodyne Research, H-ToF-AMS) driven in V mode (Drewnick et al., 2005). Particles collected through an aerodynamic lens were heated at 873 K to evaporate particulate compounds; vaporized compounds were then ionized by electron ionization and analyzed using a ToF-MS instrument with a mass resolution of ~ 2700 at m/z 28. Data obtained by H-ToF-AMS were numerically analyzed using ToF-AMS Analysis Toolkit Program Version 1.48 combined with ToF-AMS HR Analysis Program Version 1.07. Measurements of FT-IR, SMPS, and H-ToF-AMS were carried out every 10 min in Runs 1 and 4 or every 6 min in the other runs.

Off-line SOA analytical samples were collected on a Teflon membrane filter (Sumitomo Electric, Fluoropore, 47 mm diameter, pore size 1 μm). The sampling flow rate was 16.7 l min^{-1} . The sampling duration was ~ 1 h per filter. One sample for iodometric spectrophotometry was collected in each of Runs 1 and 4, or two samples (i.e., one for iodometric spectrophotometry and the other for LC/TOF-MS analysis) were collected in each of the other runs.

The time series of the OH concentration was estimated assuming that aromatic hydrocarbon decreased by the reaction with OH radicals, where the rate constants used for calculations were taken from Atkinson (1986) and Aschmann et al. (2006). In each experiment, the OH concentration reached a maximum immediately after the start of irradiation and then decreased with time, but the OH concentration maintained $> 5 \times 10^5 \text{ molecules cm}^{-3}$ during irradiation. This indicates that particles and vapors in the reaction chamber were continuously oxidized during irradiation in each experiment.

2.2 LC/TOF-MS analysis

Each filter sample was sonicated in 5 ml of methanol for 30 min to extract the collected organic compounds. The extract was concentrated to near dryness and then dissolved in 1 ml of formic acid-methanol-water solution (v/v/v = 1/2000/1999) for use as the analytical sample. Sample vials were stored in a freezer until analysis was performed.

Off-line SOA samples were analyzed by LC/TOF-MS (Agilent Technology, 6200 Series Accurate-Mass Time-of-Flight LC/MS). The mobile phases used for LC were

0.05 % v/v formic acid aqueous solution and methanol. The total flow rate of the mobile phases was 0.4 ml min^{-1} . The methanol concentration was maintained at 50 % v/v during the flow injection analysis (in which no column is used). On the other hand, for the column injection analysis, the chromatographic gradient started at 5 % v/v methanol and progressed linearly to 90 % v/v in 30 min. An octadecyl silica gel column (GL Science, ODS-3V, 0.46 mm diameter \times 150 mm long, particle size 0.5 μm) was used to separate the analytes. The temperature of the column was maintained at 298 K. The analytes were ionized by electrospray ionization (ESI) in negative polarity mode and were then analyzed using a ToF-MS instrument with a mass accuracy of < 3 ppm.

2.3 Iodometric spectrophotometry

The total amount of organic peroxide (ROOR and ROOH) present in SOA was quantified following a method established by Docherty et al. (2005). Each filter sample was sonicated in 1.5 ml ethyl acetate for 10 min to extract any organic peroxides. The extract was mixed with 2.25 ml of formic acid-chloroform-water solution (v/v/v = 53/27/20). A 3-ml aliquot of the mixture solution was then placed in a 5-ml glass vial and dry nitrogen was bubbled gently through to remove any dissolved oxygen. The mixture solution was then added with 48 mg of potassium iodide.

One hour after the addition of potassium iodide, the absorbance of the mixture solution was measured using an ultraviolet-visible spectrophotometer (Shimadzu, BioSpec-mini). The molar concentration of triiodide ions (formed from the titration reaction of organic peroxides with excess iodide ions) was determined from the absorbance at 470 nm. The molar absorption coefficient of triiodide ion used for the calculations was measured by titration with benzoyl peroxide solution at a known concentration. The molar concentration was converted to the mass concentration in a manner similar to that described by Docherty et al. (2005).

3 SOA yield

The SOA yield was determined from the SOA volume concentration and the concentration of reacted hydrocarbon (Table 1). Not all hydrocarbons were consumed in the reactions taking place during photoirradiation (Supplement Fig. S1). The concentration of reacted hydrocarbons was determined from the difference between the initial concentration and the concentration at a specific time and was then used in calculations of the SOA yield. The SOA yield was calculated when the volume concentration reached a maximum. No corrections to account for wall deposition loss of particles were performed. The volume concentration was converted to the mass concentration, assuming the density of SOA to be 1.4 g cm^{-3} (Alfarra et al., 2006; Martine-Reviejo and Wirtz, 2005).

The SOA yield increased with increasing the SOA mass loading, primarily because the gas/particle absorption of semivolatile compounds (SVOCs) increases as a result (Odum et al., 1997). The SOA mass loading increased with increasing the initial hydrocarbon or methyl nitrite concentration. Under high-concentration conditions, the yield of SVOCs will increase, because the total concentration of peroxy radicals (RO₂ and HO₂) increases (Kroll and Seinfeld, 2008). The increase in the peroxy radical concentration will also affect the increase in the SOA yield.

Martin-Reviejo and Wirtz (2005) reported the SOA yield from benzene to be 11–14 % at an SOA mass concentration of 56–94 µg m⁻³ (Fig. S2). The SOA yield reported by Ng et al. (2007) is 28 % at a mass concentration of 35 µg m⁻³. The SOA yield of Run 2 (8.0 % at 49 µg m⁻³) was lower than the previous results in the region (35–56 µg m⁻³); this is primarily because the initial NO_x concentration of Run 2 (889 ppb) was much higher than those of the previous studies (50–169 ppb). The SOA yields from 1,3,5-TMB were reported to be 3.1 % at 31 µg m⁻³ (Odum et al., 1997) and 3.6 % at 18 µg m⁻³ (Kleindienst et al., 1999). The mass loadings of the experiment by Odum et al. (1997) and Run 4 were close to each other. The SOA yield measured by Odum et al. (1997) (3.6 %) was slightly higher than the yield measured in Run 4 (2.5 %), although the NO_x level of this previous study (385 ppb) was higher than that of Run 4 (200 ppb). The yields obtained in the present study will be slightly underestimated by influence from wall deposition loss of particles and semivolatile compounds. The present and previous results showed the SOA yield from benzene to be higher than that from 1,3,5-TMB.

4 The formation and aging of organics

4.1 Van Krevelen diagram

Particulate organics and nitrates were detected when SOA was observed by H-ToF-AMS. The O/C ratio of organics increased with time, whereas the H/C ratio decreased with time (Fig. S1). Here, HR-AMS NO⁺ and NO₂⁺ ions were not included in O/C and H/C calculations, since these ions were treated as being formed from nitrates. In this study, benzene or 1,3,5-TMB does not react away completely during irradiation, which means that SOA formation and particle growth are ongoing throughout the experiments; however, the increase in the O/C ratio of particulate organics measured by H-ToF-AMS shows SOA aging occurs continuously during experiments.

A van Krevelen diagram was studied using the measured O/C and H/C ratios (Fig. 1). The oxidation state of carbon (OS_C = 2 O/C – H/C, Kroll et al., 2011) evaluated for SOA from benzene increased from –0.13 to 0.60 as SOA aged. The oxidation state of SOA from 1,3,5-TMB was –1.22 to –0.53. SOA from 1,3,5-TMB was less oxidized than with

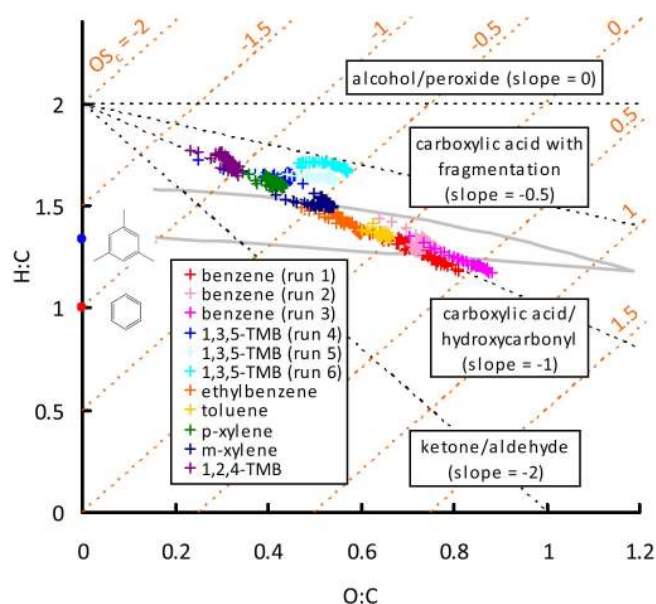


Fig. 1. Van Krevelen diagram of SOA formed from the photooxidation of aromatic hydrocarbons in the presence of NO_x; data of benzene and 1,3,5-trimethylbenzene shown with a run number are present results; data of other hydrocarbons are taken from Sato et al. (2010); data from ambient organic aerosol measurements appear in a region surrounded by gray curves (Ng et al., 2011).

benzene. The maximum oxidation state of ambient OOA is predicted to be 1.3 (Ng et al., 2011). This value was higher than the maximum of the oxidation state of SOA from benzene (0.60). The O/C ratios of start points are 0.62 (Run 1), 0.64 (Run 2), and 0.70 (Run 3) for experiments with benzene and 0.25 (Run 4), 0.27 (Run 5), and 0.31 (Run 6) for experiments with 1,3,5-TMB. It appears that increased NO_x and increased mass loading go with increasing the start point O/C ratio. The O/C ratio of SOA from aromatic hydrocarbons was shown to be independent of the NO_x level (Chhabra et al., 2011). The present results indicate that the O/C ratio of start point increases with increasing the mass loading.

In Fig. 1, the black dotted straight line with a slope of 0 represents the evolution of the H/C and O/C ratios if only alcohols or peroxides would be formed in the SOA; the black dotted straight line with a slope of –0.5, the evolution of the H/C and O/C ratios if only carboxylic acids would be produced in the SOA by fragmentation; that with a slope of –1, the evolution of the H/C and O/C ratios if only carboxylic acids or hydroxycarbonyls would be formed in the SOA; and that with a slope of –2, the evolution of the H/C and O/C ratios if only ketones or aldehydes would be formed in the SOA (Ng et al., 2011). The present data were clustered near the straight line with a slope of –1. As SOA ages, the data points migrate along this straight line, suggesting that organics present in SOA are rich in carboxylic acids or hydroxycarbonyls, and the functionalization with a carboxylic group or that with hydroxy + carbonyl groups on different carbons

proceeds during SOA aging. In the experiments with 1,3,5-TMB under high mass loading conditions (Runs 5 and 6), the data appeared in the region between the straight line with a slope of -1 and that with a slope of -0.5 , showing that increased contributions from alcohols, peroxides, and/or carboxylic acids formed as a result of fragmentation. Such a mass loading dependence is not seen for benzene data, indicating that carboxylic acid or hydroxycarbonyl formation is limited, not only due to an increase in mass loading, but also due to the reactant chemical structure.

The van Krevelen diagram of SOA from various aromatic hydrocarbons was studied using the data of Sato et al. (2010). All the data were clustered close to the straight line with a slope of -1 (Fig. 1). Chhabra et al. (2011) reported similar results for SOA from toluene and *m*-xylene. These previous results also suggest that SOA from aromatic hydrocarbons is rich in carboxylic acids or hydroxycarbonyls.

The H/C ratio of SOA from benzene (1.35–1.42) was lower than for 1,3,5-TMB (1.68–1.72); this is because the H/C ratio of precursor benzene is lower than that of 1,3,5-TMB. The H/C ratio of SOA was higher than that of its precursor. However, the H/C ratios of dicarbonyl and dicarboxylic acid formed by the ring-opening reaction of an aromatic hydrocarbon are the same as that of the precursor (e.g., muconaldehyde (C₆H₆O₂), Calvert et al., 2002, and muconic acid (C₆H₆O₄), Borrás and Tortajada-Genaro, 2012, from benzene (C₆H₆)). In SOA particles, not only ring-opened carboxylic acids but also ring-opened carbonyl hydrates (e.g., muconaldehyde hydrate (C₆H₁₀O₄)) or ring-opened alcohols (e.g., 2,4-hexadiene-1,6-diol (C₆H₁₀O₂), Borrás and Tortajada-Genaro, 2012) will be present. Further, the H/C ratio will also increase if the double bond of ring-opened products is converted to a saturated structure (e.g., succinic anhydride from toluene, Forstner et al., 1997).

The O/C ratio of SOA from benzene (0.62–0.71) was higher than that of 1,3,5-TMB (0.25–0.47). This is because very few of the methyl groups of 1,3,5-TMB are oxidized. In other words, the reactions relevant to SOA formation and aging proceed through the reactions of the aromatic ring.

4.2 LC/TOF-MS analysis

The results of LC/TOF-MS analysis of SOA collected in the experiment with benzene are shown in Table 2. To determine the ion formula, the error between the predicted m/z and the measured m/z was evaluated for probable candidates. The ion formula was identified to be the candidate with the minimum error. High-polarity products from aromatic hydrocarbons such as carboxylic acids and phenols are only detected by LC/MS in negative polarity mode (Sato et al., 2007). The chemical structure was estimated by assuming that measured ions are deprotonated ring-opened carboxylic acids or deprotonated phenolic compounds.

The ions of m/z 138 and 154 were identified, using standard reagents, as 4-nitrophenol and 4-nitrocatechol. Other

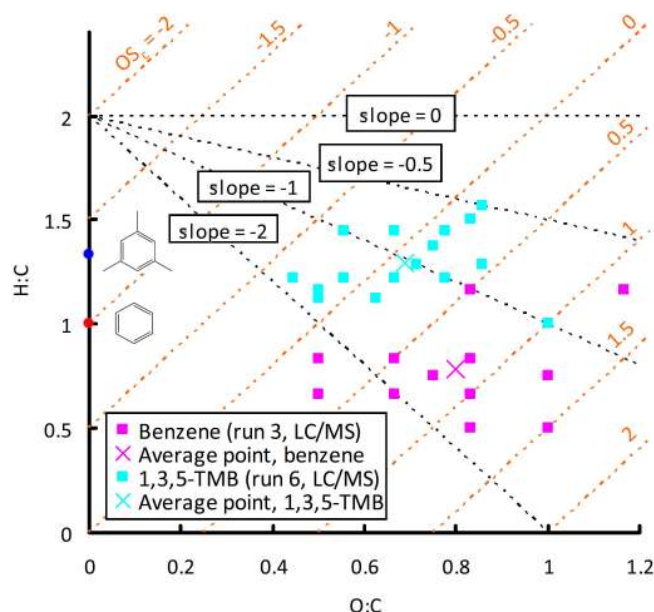


Fig. 2. Van Krevelen diagram of organic molecules identified by off-line LC/TOF-MS analysis of SOA from the photooxidation of aromatic hydrocarbons in the presence of NO_x.

ions were provisionally identified as the molecules shown in Table 2. To our knowledge, C₄H₄O₃, C₆H₆O₅, C₆H₈O₅, and C₆H₄N₂O₆ were newly identified in this study. Nitrophenol isomers, nitrocatechol isomers, C₄H₄O₄, C₆H₆O₃, C₆H₆O₄, and C₆H₅NO₅ were also identified in a recent GC/MS analysis (Borrás and Tortajada-Genaro, 2012). Ring-opened products have an aldehyde or carboxyl group at each end. Oxalic acid is known to be present in SOA from benzene (Borrás and Tortajada-Genaro, 2012). However, oxalic acid was not detected due to its high detection limit.

The results of LC/TOF-MS analysis of SOA collected in the experiment with 1,3,5-TMB are shown in Table 3. The ion of m/z 87 was identified, using standard reagents, as pyruvic acid. All the other ions were provisionally identified as the molecules shown in Table 3. The products other than pyruvic acid are, to our knowledge, newly identified. Pyruvic acid was also identified by Fisseha et al. (2004). All the identified products were ring-opened products. These products have a ketone or carboxyl group at each end. No nitrophenols were identified. Nitrophenols show absorption in the visible region of <460 nm (Calvert et al., 2002). The color of the sample filters of SOA from benzene was light yellow (Fig. S1), whereas that of sample filters of SOA from 1,3,5-TMB was white.

Figure 2 shows the van Krevelen diagram of products identified by LC/TOF-MS analysis. The arithmetic average point of products from benzene and that of products from 1,3,5-TMB appeared in a region between the straight line with a slope of -1 and that with a slope of -2 . The oxidation state of the average point of benzene (0.82) is higher than that

Table 2. LC/TOFMS measured particulate products from benzene oxidation (Run 3).

| Measured ion (<i>m/z</i>) | Retention time (min) | Suggested ion formula | Error (ppm) | Proposed structure ^a | Note |
|-----------------------------|----------------------|--|-------------|---------------------------------|------|
| 99.0080 | 2.2 | C ₄ H ₃ O ₃ [−] | 8.1 | | b |
| 115.0022 | 2.0, 4.3 | C ₄ H ₃ O ₄ [−] | 12.9 | | c |
| 125.0239 | 5.6, 7.5, 23.1 | C ₆ H ₅ O ₃ [−] | 4.9 | | d, c |
| 138.0192 | 21.7, 22.3 | C ₆ H ₄ NO ₃ [−] | 3.5 | | e, c |
| 141.0186 | 2.0, 7.0, 8.8 | C ₆ H ₅ O ₄ [−] | 5.2 | | f, c |
| 154.0145 | 18.7, 20.0, 22.8 | C ₆ H ₄ NO ₄ [−] | 0.4 | | g, c |
| 157.0138 | 1.9, 3.0, 4.1 | C ₆ H ₅ O ₅ [−] | 2.7 | | b |
| 159.0282 | 2.1 | C ₆ H ₇ O ₅ [−] | 10.7 | | b |
| 170.0093 | 15.2, 17.8, 19.0 | C ₆ H ₄ NO ₅ [−] | 1.2 | | c |
| 183.0041 | 26.6, 27.5 | C ₆ H ₃ N ₂ O ₆ [−] | 3.6 | | b |
| 191.0197 | 3.3 | C ₆ H ₇ O ₇ [−] | 0.0 | | b |
| 198.9993 | 21.9 | C ₆ H ₃ N ₂ O ₆ [−] | 1.7 | | b |

^a Structural and stereo isomers are likely; for simplicity only one isomer is shown, ^b newly identified, ^c found very recently by GC/MS analysis (Borrás et al., 2012),

^d latest-eluting compound will have cyclic structure, ^e two peaks were identified to be 2-nitrophenol and 4-nitrophenol; the signal of 4-nitrophenol (21.7 min) was stronger than the other, ^f no strong signal of trans,trans-muconic acid was found; detected peaks will be attributed to other structural isomers. The peak at 8.8 min was the highest, ^g strongest peak was identified to be 4-nitrocatechol.

determined by H-ToF-AMS for benzene SOA (0.55), where the H-ToF-AMS data were averaged during the filter sampling period only. A similar result was obtained for 1,3,5-TMB, indicating that products undetectable by the LC/TOF-MS instrument have lower oxidation states than detectable ones. On the other hand, the oxidation state of the products from benzene was higher than that of the products from

1,3,5-TMB. The results of LC/TOF-MS analysis also show a tendency for products from benzene to be more highly oxidized than those from 1,3,5-TMB.

Signals for oligomers were detected in the region *m/z* 250–600 (benzene sample) and in the region *m/z* 250–1000 (1,3,5-TMB sample) by flow injection analysis (Fig. S3). The difference in oligomer distribution is likely to result from the

Table 3. LC/TOFMS measured particulate products from 1,3,5-TMB oxidation (Run 6).

| Measured ion (<i>m/z</i>) | Retention time (min) | Suggested ion formula | Error (ppm) | Proposed structure ^a | Note |
|-----------------------------|----------------------|--|-------------|---------------------------------|------|
| 87.0080 | 6.2 | C ₃ H ₃ O ₃ [−] | 9.0 | | b, c |
| 127.0393 | 11.6, 12.1, 13.8 | C ₆ H ₇ O ₃ [−] | 6.0 | | d |
| 161.0456 | 4.6, 6.1 | C ₆ H ₉ O ₅ [−] | −0.1 | | d |
| 169.0494 | 13.2, 14.7 | C ₈ H ₉ O ₄ [−] | 7.0 | | d |
| 173.0444 | 8.0, 11.6 | C ₇ H ₉ O ₅ [−] | 6.3 | | d |
| 183.0650 | 15.0, 17.3 | C ₉ H ₁₁ O ₄ [−] | 6.8 | | d |
| 185.0444 | 8.2, 11.4 | C ₈ H ₉ O ₅ [−] | 6.0 | | d |
| 189.0405 | 7.3 | C ₇ H ₉ O ₆ [−] | 0.1 | | d |
| 191.0562 | 3.1 | C ₇ H ₁₁ O ₆ [−] | −0.3 | | d |
| 199.0597 | 14.7 | C ₉ H ₁₁ O ₅ [−] | 7.6 | | d |
| 201.0747 | 11.6, 12.1 | C ₉ H ₁₃ O ₅ [−] | 10.4 | | d |
| 203.0548 | 12.0, 12.9 | C ₈ H ₁₁ O ₆ [−] | 6.6 | | d |
| 215.0547 | 10.2, 15.9 | C ₉ H ₁₁ O ₆ [−] | 6.8 | | d |
| 217.0708 | 8.4 | C ₉ H ₁₃ O ₆ [−] | 4.4 | | d |
| 231.0507 | 13.0, 16.9, 20.8 | C ₉ H ₁₁ O ₇ [−] | 1.4 | | d |
| 233.0652 | 8.7, 16.3, 17.0 | C ₉ H ₁₃ O ₇ [−] | 6.3 | | d |

^a Structural and stereo isomers are likely; for simplicity only one isomer is shown, ^b identified to be pyruvic acid, ^c found by ion chromatograph-mass spectrometry by Fisseha et al. (2004), ^d newly identified.

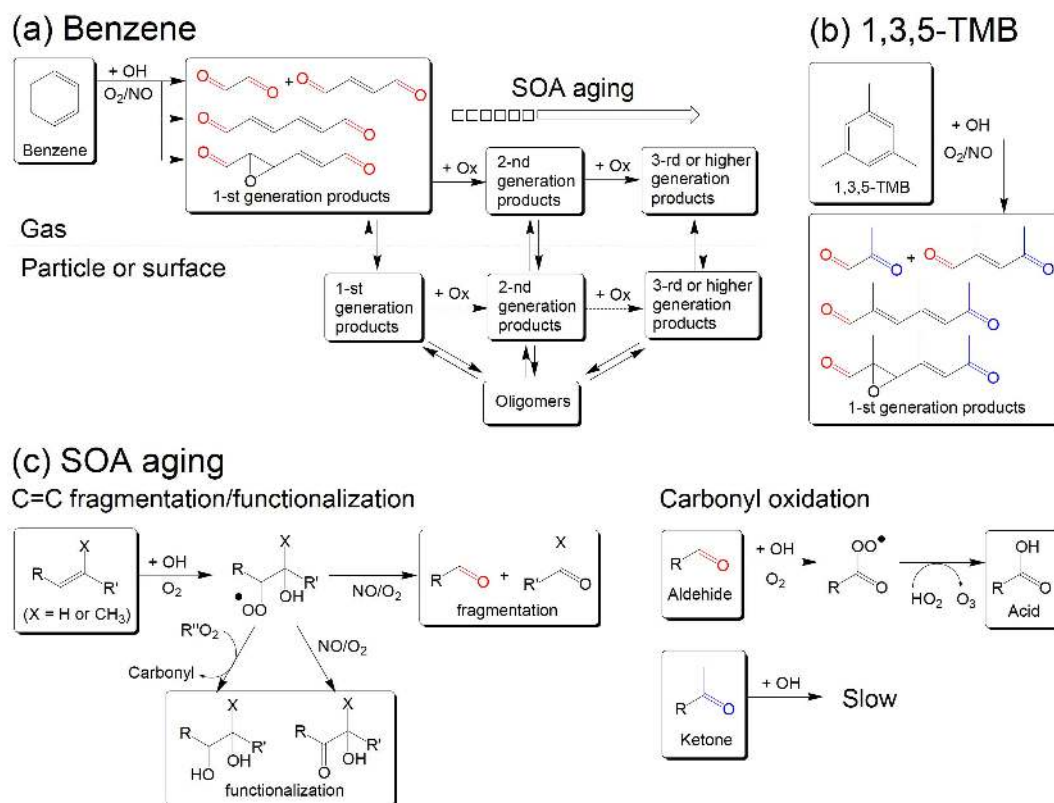


Fig. 3. Reaction schemes of (a) SOA formation from benzene photooxidation, (b) SOA formation from 1,3,5-trimethylbenzene photooxidation, and (c) SOA aging. A probable pathway to form each depicted product is only shown for simplicity; carboxylic acid can also be produced by the heterogeneous decomposition of peroxyacyl nitrates (PANs) from the acyl peroxy radical + NO₂ reaction (Surratt et al., 2010); hydroxycarbonyl produced by functionalization can also be formed by the reaction of hydroxy peroxy radical with R''O₂; hydroxy peroxy radical of the intermediate of fragmentation/functionalization can also react with HO₂; and acylperoxy radical of the intermediate of carbonyl oxidation can also react with NO or RO₂.

differences in the SOA mass loading and the chemical structure of the precursor. The signal intensities of these oligomers were lower than those of low-MW products by a factor of approximately 10². No oligomers were detected in the column injection analysis. By using H-ToF-AMS, the signals in the 200–600 region were detected in both experiments with benzene and 1,3,5-TMB (Fig. S4). These results strongly suggest that oligomers are present in SOA particles. Since carbonyls and alcohols are present in SOA particles formed from aromatic hydrocarbons, oligomers are formed from the particle phase reactions such as carbonyl hydration, acetal condensation, carbonyl polymerization, and aldol condensation (Jang and Kamens, 2001; Jang et al., 2002; Kalberer et al., 2004).

4.3 Reaction schemes for SOA formation and aging

To interpret the present results, a reaction mechanism relevant to SOA formation and aging is now discussed (Fig. 3). The major fraction of total SOA mass is believed to comprise ring-opened products from aromatic hydrocarbons (Jang and Kamens, 2001; Fisseha et al., 2004). As shown in Fig. 3a,

dialdehydes are produced as ring-opened products from the reaction of benzene with OH radicals (Calvert et al., 2002). These products, as well as second-generation products formed from subsequent oxidation, are absorbed onto existing particles. Some second-generation products have both carbonyl and hydroxy groups. In the particle phase, oligomers are formed from carbonyl hydration, acetal condensation, carbonyl polymerization, and aldol condensation (Jang and Kamens, 2001; Jang et al., 2002; Kalberer et al., 2004). The photooxidation process of 1,3,5-TMB is basically the same as for benzene (Fig. 3b). Ketoaldehydes are likely to be produced as gas-phase oxidation products.

Nakao et al. (2011) and Borrás and Tortajada-Genaro (2012) have recently reported that a substantial amount of SOA is also formed through the oxidation of phenolic products from aromatic hydrocarbons. As oxidation products from phenols, ring-opened molecules such as glyoxal + butenedial and hydroxylated compounds of these are formed (Bloss et al., 2005). Ring-opened products from phenolic compounds will also contribute to SOA formation.

The present results indicate that SOA aging proceeds through the oxidation of the internal double bond of ring-opened products and carboxylic acid formation resulting from the oxidation of the carbonyl group (Fig. 3c). Loza et al. (2012) suggested that SOA aging in laboratory chamber experiments proceeds through the gas-phase oxidation of SVOCs, although oxidation on particle surfaces cannot be excluded. The gas-phase oxidation of the internal double bond results in fragmentation or functionalization. As a result of fragmentation, a carbonyl pair is formed. These carbonyls then undergo the following oxidation. The functionalization of the internal carbons of ring-opened products produces hydroxycarbonyls or diols; these reactions affect the increase in the O/C ratio (van Krevelen diagram), but will not affect the increase in the m/z 44 signal (triangle plot).

Gas-phase carboxylic acid formation from carbonyls is initiated by reactions with OH radicals. Generally, the reactions of ketones with OH radicals are slower than the reactions of aldehydes. For example, the lifetime of acetaldehyde is 20 h at an OH concentration of 10^6 molecules cm^{-3} , whereas that of acetone is 53 days (DeMore et al., 1997). Ketoaldehydes are produced by the reaction of 1,3,5-TMB. Since the oxidation of ketone groups is slow, formation of dicarboxylic acids from ketoaldehyde products is much slower than from dialdehyde products of benzene. Therefore, AMS measurements of SOA from benzene give stronger m/z 44 signals than those of SOA from 1,3,5-TMB (Sato et al., 2010). The ketone groups of the products from 1,3,5-TMB resist oxidation. AMS measurements of SOA from 1,3,5-TMB give stronger m/z 43 signals than those of SOA from benzene.

If carbonyl products of benzene and 1,3,5-trimethylbenzene oxidation must undergo subsequent gas-phase oxidation to carboxylic acids to decrease their vapor pressures and allow them to condense and form SOA, then this oxidation to form carboxylic acids should be classified as a SOA formation mechanism. Oxocarboxylic acids react with alcoholic products in the particle phase to form hemiacetal dimers. The reverse reactions of hemiacetal formation can occur to form oxocarboxylic acids and alcoholic products again. Particulate oxocarboxylic acids can proceed to the vaporization followed by the oxidation in the gas phase to form dicarboxylic acids, which can be absorbed on particles again, or particulate oxocarboxylic acids can be oxidized in the particle phase to form dicarboxylic acids. This oxidation to form carboxylic acids results in an increase in the O/C ratio of organics and should be classified as a SOA aging mechanism.

The SOA yield from benzene was higher than that from highly methylated 1,3,5-TMB. Sato et al. (2011) reported that the SOA yield from a highly methylated conjugated diene is much lower than that from non-methylated 1,3-butadiene. This previous result mirrors the present results for aromatic hydrocarbons. Oligoesters contribute to SOA formation during the reactions of conjugated dienes (Surratt et

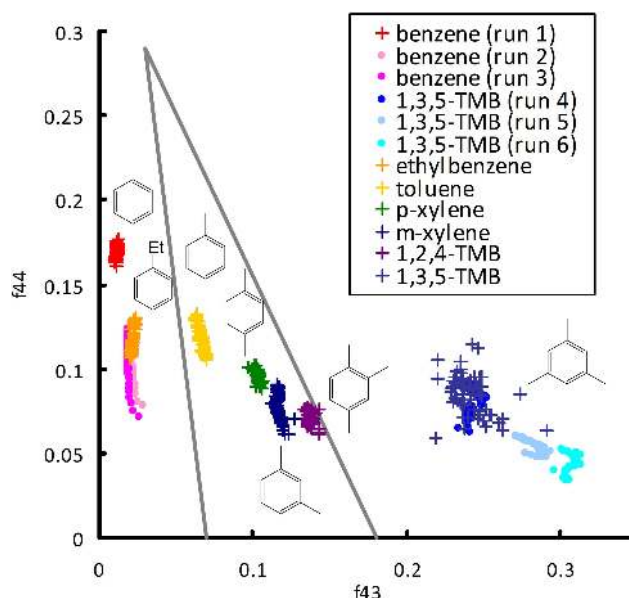


Fig. 4. Triangle plot of SOA formed from the photooxidation of aromatic hydrocarbons in the presence of NO_x; data of benzene and 1,3,5-TMB shown with a run number are present results; other data of six aromatic hydrocarbons are taken from Sato et al. (2010); cross symbol data (+) are obtained at the initial NO_x concentrations of ~ 100 ppb.

al., 2006). Ester-type oligomers will also be produced by the reactions of carboxylic acids with alcohols in the particle phase during the oxidation of aromatic hydrocarbons.

4.4 Triangle plot

The ion signals of m/z 43 and 44 originate chiefly from carbonyls and carboxylic acids, respectively (Ng et al., 2010, 2011). Strong ion signals appeared at m/z 43 and 44 in the mass spectra measured by H-TOF-AMS for SOA. The ion signal of m/z 44 was higher than m/z 43 when SOA from benzene was measured, whereas the ion signal of m/z 43 was higher than m/z 44 when SOA from 1,3,5-TMB was measured (Fig. S5). These results confirm the findings previously reported by Sato et al. (2010).

The ratio of m/z 44 to total organic aerosol (f_{44}) was plotted as a function of f_{43} to study the triangle plot proposed by Ng et al. (2010) (Fig. 4). According to Ng et al. (2010), the data for ambient organic aerosol appear in the triangle region shown in the Figure. The f_{44} value increases as aging proceeds, and peaks at 0.3. The data obtained for SOA in this study also migrated over time, toward the top of the triangle.

In the experiments with benzene, the value of f_{44} was 0.16–0.17 (Run 1) and 0.07–0.13 (Runs 2 and 3). In the experiments with 1,3,5-TMB, the value of f_{44} was 0.06–0.09 (Run 4) and 0.03–0.06 (Runs 5 and 6). The f_{44} value was constant or increased with decreasing the SOA mass loading. This tendency parallels a previous result for SOA

from α -pinene ozonolysis by Shilling et al. (2009). Particles are rich in high-volatility SVOCs at high mass loading. The present and previous results indicate that the f_{44} values of low-volatility SOVCs are higher than those of high-volatility SVOCs. Low-volatility SVOCs found in SOA from α -pinene ozonolysis are multifunctional species such as dicarboxylic acids (Shilling et al., 2009). Dicarboxylic acids were also found to be present in SOA from the benzene photooxidation. As described in the section of van Krevelen diagram, the O/C ratio of start point increased with increasing the mass loading; this trend is opposite to the relationship between the f_{44} value and the mass loading. These results suggest that the O/C ratio of the organics present in high mass loading SOA is determined by the amount of the oxygenated organics other than carboxylic acids.

Previous data measured by Sato et al. (2010) for SOA from aromatic hydrocarbons are also plotted in Fig. 4. These data were re-analyzed using a new fragment table. The intensities of m/z 18 and 28 organic fragments were modified in the new table (Aiken et al., 2008); results of f_{44} decreased $<2\%$ by this modification. Cross symbol data shown in Fig. 4 are those obtained at the initial NO_x concentrations of ~ 100 ppb. The mass loadings measured for the cross symbol data are $2\text{--}32\text{ }\mu\text{g m}^{-3}$. The f_{44} value of SOA from benzene was higher than that of SOA from 1,3,5-TMB. Despite benzene being a higher volatility precursor compared to the other aromatics with additional methyl groups, the higher volatility precursors generate the highly oxidized, presumably low volatility products. Similar results have been reported by Sato et al. (2010) and Chhabra et al. (2011), and indicate that SOA from benzene is rich in carboxylic acids. A trade-off relationship was evident between the decrease in the f_{43} value and the increase in the f_{44} value, indicating that carboxylic acids are formed from the oxidation of carbonyls. The triangle plot may also be used in other reaction systems as a tool to identify the carbonyl to acid oxidation route.

Not all data obtained in the present and previous studies appeared in the triangular region shown in Fig. 4. However, this is not unusual, since OOA observed in the ambient atmosphere is a mixture of oxidation products from various organic compounds (Chhabra et al., 2010, 2011). The f_{44} value of SOA from benzene, the highest among the plotted data, was lower than the f_{44} value at the top of the triangle region. The present results support previous findings that SOA formed from VOC oxidation in laboratory chambers is less oxidized than that of ambient OOA (Bahreini et al., 2005; Alfarra et al., 2006; Chhabra et al., 2010).

4.5 Iodometric spectrophotometry

Organic peroxides formed from the reactions of RO₂ with HO₂ are believed to contribute to SOA formation (Johnson et al., 2004, 2005; Sato et al., 2007; Ng et al., 2007; Kroll and Seinfeld, 2008). Organic peroxides appear to contribute to SOA aging, because they can function as initiators of

particle-phase radical reactions (Sato et al., 2007; Chen et al., 2011), and function as oxidants of other compounds in the aqueous phase (Wang et al., 2011). Organic peroxides might also affect the f_{44} value obtained by AMS. In this study, the ratio of organic peroxides to total SOA mass was determined by means of iodometric spectrophotometry.

The present analytical method was checked by quantifying the organic peroxides present in SOA from the ozonolysis of α -pinene. The ratio of organic peroxides to total SOA mass was determined as $45 \pm 16\%$ ($n = 8$, error 2σ). This value closely agrees with the value in the literature arrived at by Docherty et al. (2005) ($47 \pm 24\%$).

From experiments with 1,3,5-TMB, the ratio of organic peroxides to total SOA mass was determined to be $12 \pm 8\%$ ($n = 3$, error 2σ). This value is close to a previous value reported by Sato et al. (2007) for toluene SOA ($16\text{--}18\%$). Although we also measured this value in the experiments with benzene, the SOA sample obtained was not sufficiently large to permit quantification. The ratio of organic peroxides to total SOA mass was estimated, from the value of the detection limit (3σ), to be $<39\%$.

The organic peroxide to SOA ratios measured for the photooxidation of aromatic hydrocarbons in this study were lower than those measured for the ozonolysis of α -pinene. If organic peroxides affect the f_{44} value obtained by AMS, the f_{44} values of SOA from aromatic hydrocarbons would be lower than those of SOA from α -pinene. However, the f_{44} values measured in this study ($0.038\text{--}0.17$) were close to or higher than those for SOA from the α -pinene ozonolysis (0.042 , Bahreini et al., 2005). Although organic peroxides from aromatic hydrocarbon are present in SOA, the effect of these peroxides on the f_{44} data will be limited.

5 Nitrate formation

LC/TOF-MS analysis revealed no nitrophenols in SOA from 1,3,5-TMB, although they were detected in SOA from benzene. Nitrophenols appear to affect the optical properties of aerosol particles (Nakayama et al., 2010; Zhang et al., 2011) and the toxicity of aerosol particles (Furuta et al., 2004; Li et al., 2006). In addition, nitrophenols will be used as markers of ambient SOA from fossil fuels and biomass burning (Irei et al., 2006, 2011; Iinuma et al., 2010). Formation of nitrophenols from aromatic hydrocarbons is further discussed in this section.

5.1 HRNO₃/HROrg ratio

Particulate nitrophenols are detected as nitrates by AMS (Bahreini et al., 2005; Sato et al., 2010). The ratio of nitrates (HRNO₃) to organics (HROrg), identified from high-resolution mass spectra, was plotted as a function of time (Fig. 5). The NO⁺/NO₂⁺ ratio observed was $3.8\text{--}5.8$, higher than that for inorganic nitrates, indicating that the nitrates

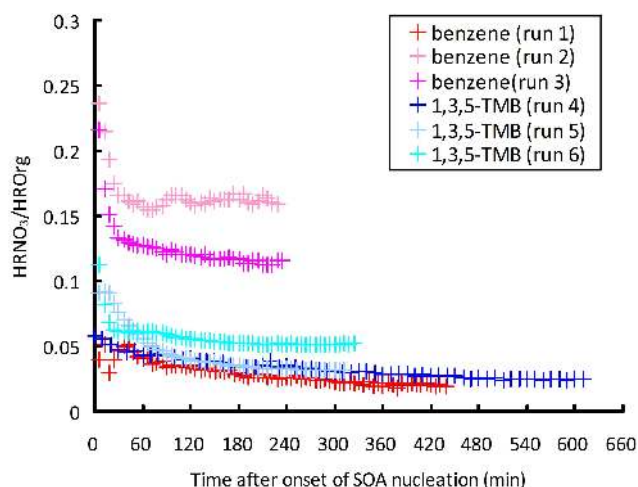


Fig. 5. Time profiles of HRNO₃/HROrg ratio measured during the photooxidation of benzene and 1,3,5-trimethylbenzene in the presence of NO_x. The background of HRNO₃ is very small as shown in Fig. S1a, so the start value of the HRNO₃/HROrg ratio is not influenced by any background signal.

observed are rich in organic nitrates or nitro organics. Since the absolute concentration of HRNO₃ determined for organonitrates is incorrect (Farmer et al., 2010), only relative comparisons are made here. The HRNO₃/HROrg ratio decreased with time. This shows that nitrophenols and organic nitrates decrease as a result of chemical reactions. The decay rate of the HRNO₃/HROrg ratio was also influenced by the faster increase in HROrg than HRNO₃ in the 0–60 min region. The average decay rate, determined from data in the region of >60 min, was 0.059 h^{−1}. If we ignore reactions in the aqueous phase, a major sink of nitrophenols and organic nitrates is photolysis in the gas phase (Calvert et al., 2002; Finlayson-Pitts and Pitts, 2000). If gaseous nitrophenols decrease by the photolysis, particulate nitrophenols are vaporized to maintain the equilibrium of gas/particle partitioning. The photolysis of gaseous nitrophenols result in a decrease in the concentration of particulate nitrophenols.

The HRNO₃/HROrg ratio measured in the experiment with benzene (Run 2) was higher than that measured in the other experiment (Run 1) in the region of >60 min; this is because the initial NO_x concentration in Run 2 (889 ppb) is higher than that for Run 1 (102 ppb). Since nitrophenols and organic nitrates are semivolatile compounds, the HRNO₃/HROrg ratio would also depend on the SOA mass loading. However, the HRNO₃/HROrg ratio measured in Run 3 ([SOA] = 198 μg m^{−3}) was close to or slightly below that measured in Run 2 ([SOA] = 49 μg m^{−3}). Under the present experimental conditions, the HRNO₃/HROrg ratio was closely dependent on the initial NO_x concentration. Very recently, we measured the HRNO₃/HROrg ratio of SOA from the toluene photooxidation as a function of initial NO_x concentration and found that the HRNO₃/HROrg

ratio increased with increasing the initial NO_x level in the range 100–600 ppb (Nakayama et al., 2012). This supports the present conclusion.

The HRNO₃/HROrg ratio also decreased in experiments with 1,3,5-TMB. The HRNO₃/HROrg ratio measured in the region >60 min (0.03–0.06) was almost independent of the initial NO_x concentration or the SOA mass loading. The NO_x concentration and the SOA mass loading in the experiment with benzene (Run 3) were close to those in the experiment with 1,3,5-TMB (Run 5). In a comparison between these experiments, the HRNO₃/HROrg ratio measured in the experiment with benzene was higher than that measured in the experiment with 1,3,5-TMB.

5.2 Reaction schemes for nitrophenol formation

To be able to interpret the relationship between the structure of aromatic hydrocarbons and the yield of nitrophenols, the reaction mechanisms relevant to formation of nitrophenols from benzene and 1,3,5-TMB were investigated (Fig. 6). These mechanisms are based on an already known reaction mechanism (Forstner et al., 1997). Phenol is produced by the reaction of benzene with OH radicals (Fig. 6a). Phenoxy radicals formed from the following oxidation process of phenol have two other resonance structures: 2-oxo-3,5-cyclohexadienyl and 4-oxo-2,5-cyclohexadienyl. The addition of NO₂ to 2-oxo-3,5-cyclohexadienyl radicals followed by isomerization results in the formation of 2-nitrophenol. Similarly, 4-nitrophenol is formed from the reaction of 4-oxo-2,5-cyclohexadienyl with NO₂.

As shown in Fig. 6b, 2,4,6-trimethylphenol is formed from the reaction of 1,3,5-TMB with OH radicals (Calvert et al., 2002; Kleindienst et al., 1999). The resonance structures of phenoxy-type radicals from this phenolic product are 1,3,5-trimethyl-2-oxo-3,5-cyclohexadienyl and 1,3,5-trimethyl-4-oxo-2,5-cyclohexadienyl. In both these structures, the carbon atom at the radical's center is bonded with a methyl group. Even if NO₂ is added to these radicals, these adducts are likely to dissociate to reactants again since subsequent isomerization involving the methyl group migration cannot take place.

Noda et al. (2009) recently reported a phenol formation pathway from alkylbenzene via dealkylation. Their results indicate that 3,5-dimethylphenol is also produced by the reaction of 1,3,5-TMB with OH radicals. The oxidation of this phenolic compound would appear to lead to the formation of 3,5-dimethyl-2-nitrophenol and 2,5-dimethyl-4-nitrophenol; however, no nitrophenols were detected in SOA from 1,3,5-TMB. The present results suggest that the yield of 3,5-dimethylphenol is lower than that of 2,4,6-trimethylphenol, or that NO₂ addition to the phenoxy from 3,5-dimethylphenol is blocked by steric hindrance.

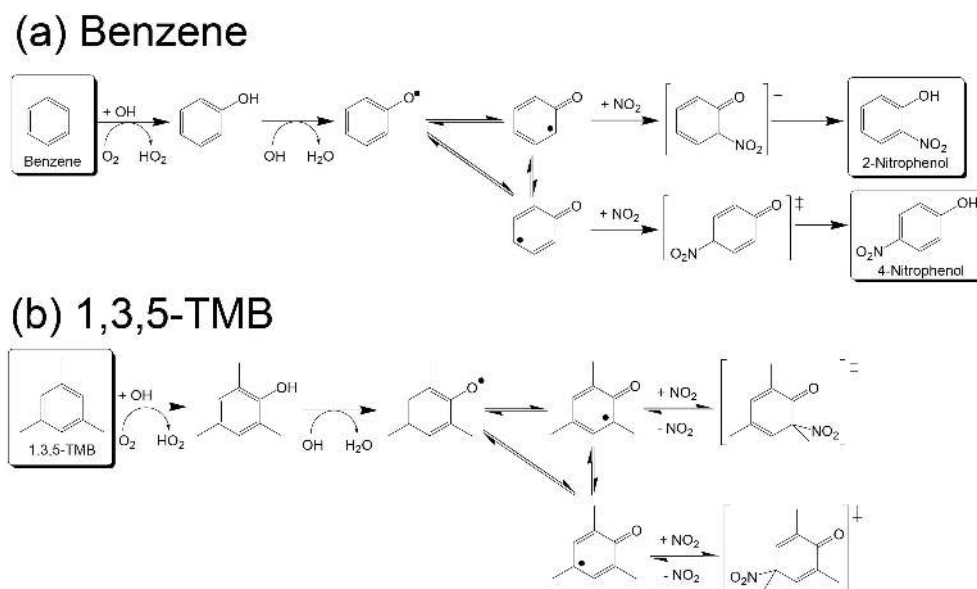


Fig. 6. Reaction schemes of (a) nitrophenol formation from the photooxidation of benzene and (b) corresponding routes from the photooxidation of 1,3,5-trimethylbenzene.

6 Comparison between chamber and ambient conditions

The present results show that laboratory SOA is less oxidized than ambient OOA, and that the rate of SOA aging in laboratory chambers is limited by the oxidation of ketone groups. Ketocarboxylic acids are also detected in ambient organic aerosol. The ratio of ketocarboxylic acids to dicarboxylic acids is known to decrease as an aerosol ages (Ho et al., 2005, 2007; He et al., 2010). These field results show that the oxidation of ketocarboxylic acids is competitive with the deposition of particles (the lifetime due to deposition is about 14 days). The rate of the oxidation of ketocarboxylic acids in the ambient atmosphere cannot be fully explained by oxidation in the gas phase.

Recently, Loza et al. (2012) carried out long-photoirradiation (>12 h) laboratory chamber experiments to investigate the photooxidation of *m*-xylene. They reported the rate of increase of the O/C ratio to be 0.0012 h⁻¹ during SOA aging. The time needed for the O/C ratio to increase from the initial SOA value (0.6) to the ambient maximum (1.2) is estimated to be 20 days. In their experiments, the chamber was continuously irradiated, suggesting that it takes a much longer time for the O/C ratio to increase to 1.2 under ambient-like intermittent irradiation conditions.

As another oxidation process of ketocarboxylic acids, oxidation in the particle phase is also possible. However, dry SOA particles are suggested to be in the amorphous solid state (Virtanen et al., 2010) or in the semi-solid phase (Shiraiwa et al., 2011). If these claims are correct, particle-phase reactions can only occur near the surface. The major fraction of total SOA mass comprises the molecules present in the in-

ternal region of particles, which remain unoxidized. On the other hand, under highly humid conditions, cloud processing such as acid-catalyzed reactions in the aqueous phase (Böge et al., 2006) and OH radical reactions in the aqueous phase (Lim et al., 2005; Carlton et al., 2006, 2007; Myriokefalitakis et al., 2011) can occur. Due to OH radical reactions in the aqueous phase, ketocarboxylic acids such as pyruvic acid can be oxidized to form dicarboxylic acids such as oxalic acid. SOA produced in laboratory chamber experiments is less oxidized than for ambient OOA, not only because the experimental duration is insufficient or the SOA mass loading in the chamber is higher than that of the atmosphere: the laboratory chamber experiments under dry conditions cannot simulate the reactions of organics in the aqueous phase that take place in cloud processing.

7 Conclusions

In this study, SOA formed from the photooxidation of benzene and 1,3,5-TMB in the presence of NO_x was measured by SMPS, H-ToF-AMS, and LC/TOF-MS. The SOA yield from benzene was higher than that from 1,3,5-TMB. A triangle plot of SOA from aromatic hydrocarbons was studied using the *f*₄₃ and *f*₄₄ data obtained by H-ToF-AMS measurements made in the present and previous studies. The *f*₄₄ value of SOA from benzene was higher than that of SOA from 1,3,5-TMB. The triangle plot also revealed a trade-off relationship between decreased *f*₄₄ value and increased *f*₄₃ value. All *f*₄₄ values obtained for SOA from aromatic hydrocarbons were lower than those of highly oxidized ambient OOA. The van Krevelen diagram plotted using AMS data for

SOA from benzene and 1,3,5-TMB showed the organic compounds present in SOA to be rich in carboxylic acids or hydroxycarbonyls. Ring-opened carboxylic acids and nitrophenols were identified as products present in SOA by LC/TOF-MS analysis of SOA from benzene. The ring-opened carboxylic acids from benzene had an aldehyde or carboxyl group at each end. On the other hand, the ring-opened carboxylic acids from 1,3,5-TMB had a ketone and carboxyl group at each end. The present results of the triangle plot, van Krevelen diagram, and composition analysis at the molecular level together indicate that SOA aging proceeds chiefly through carboxylic acid formation via the oxidation of carbonyls, and that the rate of SOA aging in laboratory chamber experiments is limited by the rate of oxidation of ketones. SOA produced in laboratory chamber experiments is less oxidized than with ambient OOA, not only because the experimental duration is insufficient or the SOA mass loading in the chamber is higher than that of the atmosphere, but because the laboratory chamber experiments under dry conditions are unable to simulate ketocarboxylic acid photochemical oxidation in the aqueous phase. In the future, understanding of aqueous-phase SOA chemistry is necessary.

The HRNO₃/HROrg ratio (representing the relative mass fraction of organonitrates or nitro organics) measured by H-ToF-AMS for SOA from benzene was confirmed to be higher than that measured for SOA from 1,3,5-TMB. The suppression of nitrophenol formation from 1,3,5-TMB is explained by the already-known reaction mechanism in relation to nitrophenol formation.

Supplementary material related to this article is available online at: <http://www.atmos-chem-phys.net/12/4667/2012/acp-12-4667-2012-supplement.pdf>.

Acknowledgements. This work was supported by a Grant-in-Aid for Scientific Research from the Japan Society for the Promotion of Science (No. 21510023, FY2009–2011). K. S. thanks K. Tanabe and Y. Takazawa at the National Institute for Environmental Studies for their assistance with LC/TOF-MS analysis. K. S. thanks T. Nakayama of Nagoya University for useful discussion on the reaction mechanism of nitrophenol formation.

Edited by: J. H. Seinfeld

References

- Aiken, A. C., DeCarlo, P. F., Kroll, J. H., Worsnop, D. R., Huffman, J. A., Docherty, K. S., Ulbrich, I. M., Mohr, C., Kimmel, J. R., Sueper, D., Sun, Y., Zhang, Q., Trimborn, A., Northway, M., Ziemann, P. J., Ganagaratna, M. R., Onasch, T. B., Alfarra, M. R., Prevot, A. S. H., Dommen, J., Duplissy, J., Metzger, A., Baltensperger, U., and Jimenez, J. L.: O/C and OM/OC ratios of primary, secondary, and ambient organic aerosols with high-resolution time-of-flight aerosol mass spectrometry, *Environ. Sci. Technol.*, 42, 4478–4485, 2008.
- Akimoto, H., Hoshino, M., Inoue, G., Sakamaki, F., Washida, N., and Okuda, M.: Design and characterization of the evacuable and bakable photochemical smog chamber, *Environ. Sci. Technol.*, 13, 471–475, 1979.
- Alfarra, M. R., Paulsen, D., Gysel, M., Garforth, A. A., Dommen, J., Prévôt, A. S. H., Worsnop, D. R., Baltensperger, U., and Coe, H.: A mass spectrometric study of secondary organic aerosols formed from the photooxidation of anthropogenic and biogenic precursors in a reaction chamber, *Atmos. Chem. Phys.*, 6, 5279–5293, doi:10.5194/acp-6-5279-2006, 2006.
- Aschmann, S. M., Long, W. D., and Atkinson, R.: Temperature-dependent rate constants for the gas-phase reactions of OH radicals with 1,3,5-trimethylbenzene, triethyl phosphate, and a series of alkylphosphonates, *J. Phys. Chem. A*, 110, 7393–7400, 2006.
- Atkinson, R.: Kinetics and mechanisms of the gas-phase reactions of the hydroxyl radical with organic compounds under atmospheric conditions, *Chem. Rev.*, 86, 69–201, 1986.
- Bahreini, R., Keywood, M. D., Ng, N. L., Varutbangkul, V., Gao, S., Flagan, R. C., Seinfeld, J. H., Worsnop, D. R., and Jimenez, J. L.: Measurements of secondary organic aerosol from oxidation of cycloalkenes, terpenes, and m-xylene using an Aerodyne Aerosol Mass Spectrometer, *Environ. Sci. Technol.*, 39, 5674–5688, 2005.
- Baltensperger, U., Dommen, J., Alfarra, M. R., Duplissy, J., Gaeggeler, K., Metzger, A., Facchini, M. C., Decesari, S., Finessi, E., Reinnig, C., Schott, M., Warnke, J., Hoffmann, T., Klatzer, B., Puxbaum, H., Geiser, M., Savi, M., Lang, D., Kalberer, M., and Geiser, T.: Combined determination of the chemical composition and of health effects of secondary organic aerosols: the POLYSOA project, *J. Aerosol Med. Pulm. D.*, 21, 145–154, 2008.
- Bloss, C., Wagner, V., Jenkin, M. E., Volkamer, R., Bloss, W. J., Lee, J. D., Heard, D. E., Wirtz, K., Martin-Reviejo, M., Rea, G., Wenger, J. C., and Pilling, M. J.: Development of a detailed chemical mechanism (MCMv3.1) for the atmospheric oxidation of aromatic hydrocarbons, *Atmos. Chem. Phys.*, 5, 641–664, doi:10.5194/acp-5-641-2005, 2005.
- Böge, O., Miao, Y., Plewka, A., and Herrmann, H.: Formation of secondary organic particle phase compounds from isoprene gas-phase oxidation products: an aerosol chamber and field study, *Atmos. Environ.*, 40, 2501–2509, 2006.
- Borrás, E. and Tortajada-Genaro, L. A.: Secondary organic aerosol formation from the photo-oxidation of benzene, *Atmos. Environ.*, 47, 154–163, 2012.
- Calvert, J. G., Atkinson, R., Becker, K. H., Kamens, R. M., Seinfeld, J. H., Wallington, T. J., and Yarwood, G.: *The Mechanisms of Atmospheric Oxidation of Aromatic Hydrocarbons*, Oxford University Press, New York, USA, 2002.
- Carlton, A. G., Turpin, B. J., Lim, H.-J., Altieri, K. E., and Seitzinger, S.: Link between isoprene and secondary organic aerosol (SOA): Pyruvic acid oxidation yields low volatility organic acids in clouds, *Geophys. Res. Lett.*, 33, L06822, doi:10.1029/2005GL025374, 2006.
- Carlton, A. G., Turpin, B. J., Altieri, K. E., Seitzinger, S., Reff, A., Lim, H.-J., and Ervens, B.: Atmospheric oxalic acid and SOA production from glyoxal: Results of aqueous photooxidation experiments, *Atmos. Environ.*, 41, 7588–7602, 2007.

- Chen, Q., Liu, Y., Donahue, N. M., Shilling, J. E., and Martin, S. T.: Particle-phase chemistry of secondary organic material: modeled compared to measured O:C and H:C elemental ratios provide constraints, *Environ. Sci. Technol.*, 45, 4763–4770, 2011.
- Chhabra, P. S., Flagan, R. C., and Seinfeld, J. H.: Elemental analysis of chamber organic aerosol using an aerodyne high-resolution aerosol mass spectrometer, *Atmos. Chem. Phys.*, 10, 4111–4131, doi:10.5194/acp-10-4111-2010, 2010.
- Chhabra, P. S., Ng, N. L., Canagaratna, M. R., Corrigan, A. L., Russell, L. M., Worsnop, D. R., Flagan, R. C., and Seinfeld, J. H.: Elemental composition and oxidation of chamber organic aerosol, *Atmos. Chem. Phys.*, 11, 8827–8845, doi:10.5194/acp-11-8827-2011, 2011.
- DeMore, W. B., Sander, S. P., Golden, D. M., Hampson, R. F., Kurylo, M. J., Howard, C. J., Ravishankara, A. R., Kolb, C. E., and Molina, M. J.: Chemical kinetics and photochemical data for use in stratospheric modeling, Evaluation number 12, JPL Publication, 97-4, 1–266, 1997.
- Docherty, K. S., Wu, W., Lim, Y. B., and Ziemann, P. J.: Contributions of organic peroxides to secondary aerosol formed from reactions of monoterpenes with O₃, *Environ. Sci. Technol.*, 29, 4049–4059, 2005.
- Drewnick, F., Hings, S. S., DeCarlo, P. F., Jayne, J. T., Gonin, M., Fuhrer, K., Weimer, S., Jimenez, J. L., Demerjian, K. L., Borrmann, S., and Worsnop, D. R.: A new time-of-flight aerosol mass spectrometer (ToF-AMS) – instrument description and first field deployment, *Aerosol Sci. Tech.*, 39, 637–658, 2005.
- Farmer, D. K., Matsunaga, A., Docherty, K. S., Surratt, J. D., Seinfeld, J. H., Ziemann, P. J., and Jimenez, J. L.: Response of an aerosol mass spectrometer to organonitrates and organosulfates and implications for atmospheric chemistry, *P. Natl. Acad. Sci. USA*, 107, 6670–6675, 2010.
- Finlayson-Pitts, B. J. and Pitts, J. N.: *Chemistry of the Upper and Lower Atmosphere – Theory, Experiments, and Applications*, Academic Press, San Diego, California, USA, 2000.
- Fisseha, R., Dommen, J., Sax, M., Paulsen, D., Kalberer, M., Maurer, R., Höfler, F., Weingartner, E., and Baltensperger, U.: Identification of organic acids in secondary organic aerosol and the corresponding gas phase from chamber experiments, *Anal. Chem.*, 76, 6535–6540, 2004.
- Forstner, H. J. L., Flagan, R. C., and Seinfeld, J. H.: Secondary organic aerosol from the photooxidation of aromatic hydrocarbons: Molecular composition, *Environ. Sci. Technol.*, 31, 1345–1358, 1997.
- Furuta, C., Suzuki, A. K., Taneda, S., Kamata, K., Hayashi, H., Mori, Y., Li, C., Watanabe, G., and Taya, K.: Estrogenic activities of nitrophenols in diesel exhaust particles, *Biol. Reprod.*, 70, 1527–1533, 2004.
- Hallquist, M., Wenger, J. C., Baltensperger, U., Rudich, Y., Simpson, D., Claeys, M., Dommen, J., Donahue, N. M., George, C., Goldstein, A. H., Hamilton, J. F., Herrmann, H., Hoffmann, T., Iinuma, Y., Jang, M., Jenkin, M. E., Jimenez, J. L., Kiendler-Scharr, A., Maenhaut, W., McFiggans, G., Mentel, Th. F., Monod, A., Prévôt, A. S. H., Seinfeld, J. H., Surratt, J. D., Szmigielski, R., and Wildt, J.: The formation, properties and impact of secondary organic aerosol: current and emerging issues, *Atmos. Chem. Phys.*, 9, 5155–5236, doi:10.5194/acp-9-5155-2009, 2009.
- Hamilton, J. F., Webb, P. J., Lewis, A. C., and Reviejo, M. M.: Quantifying small molecules in secondary organic aerosol formed during the photo-oxidation of toluene with hydroxyl radicals, *Atmos. Environ.*, 39, 7263–7275, 2005.
- He, N. and Kawamura, K.: Distributions and diurnal changes of low molecular weight organic acids and alpha-dicarbonyls in suburban aerosols collected at Mangshan, North China, *Geochem. J.*, 44, E17–E22, 2010.
- Henze, D. K., Seinfeld, J. H., Ng, N. L., Kroll, J. H., Fu, T.-M., Jacob, D. J., and Heald, C. L.: Global modeling of secondary organic aerosol formation from aromatic hydrocarbons: high- vs. low-yield pathways, *Atmos. Chem. Phys.*, 8, 2405–2420, doi:10.5194/acp-8-2405-2008, 2008.
- Ho, K. F., Lee, S. C., Cao, J. J., Kawamura, K., Watanabe, T., Cheng, Y., and Chow, J. C.: Dicarboxylic acids, ketocarboxylic acids and dicarbonyls in the urban roadside area of Hong Kong, *Atmos. Environ.*, 40, 3030–3040, 2005.
- Ho, K. F., Cao, J. J., Lee, S. C., Kawamura, K., Zhang, R. J., Chow, J. C., and Watson, J. G.: Dicarboxylic acids, ketocarboxylic acids, and dicarbonyls in the urban atmosphere of China, *J. Geophys. Res.*, 112, D22S27, doi:10.1029/2006JD008011, 2007.
- Hu, D., Tolocka, M., Li, Q., and Kamens, R. M.: A kinetic mechanism for predicting secondary organic aerosol formation from toluene oxidation in the presence of NO_x and natural sunlight, *Atmos. Environ.*, 41, 6478–6496, 2007.
- Huang, M., Zhang, W., Hao, L., Wang, Z., Zhao, W., Gu, X., Guo, X., Liu, X., Long, B., and Fang, L.: Laser desorption/ionization mass spectrometric study of secondary organic aerosol formed from the photooxidation of aromatics, *J. Atmos. Chem.*, 58, 237–252, 2007.
- Hurley, M. D., Sokolov, O., Wallington, T. J., Takekawa, H., Karasawa, M., Klotz, B., Barnes, I., and Becker, K. H.: Organic aerosol formation during the atmospheric degradation of toluene, *Environ. Sci. Technol.*, 35, 1358–1366, 2001.
- Iinuma, Y., Böge, O., Gräfe, R., and Herrmann, H.: Methyl-nitrocatechols: atmospheric tracer compounds for biomass burning secondary organic aerosols, *Environ. Sci. Technol.*, 44, 8453–8459, 2010.
- Irei, S., Huang, L., Collin, F., Zhang, W., Hastie, D., and Rudolph, J.: Flow reactor studies of the stable carbon isotope composition of secondary particulate organic matter generated by OH-radical-induced reactions of toluene, *Atmos. Environ.*, 40, 5858–5867, 2006.
- Irei, S., Rudolph, J., Huang, L., Auld, J., and Hastie, D.: Stable carbon isotope ratio of secondary particulate organic matter formed by photooxidation of toluene in indoor smog chamber, *Atmos. Environ.*, 45, 856–862, 2011.
- Izumi, K. and Fukuyama, T.: Photochemical aerosol formation from aromatic hydrocarbons in the presence of NO_x, *Atmos. Environ.*, 24A, 1433–1441, 1990.
- Jang, M. and Kamens, R. M.: Characterization of secondary aerosol from the photooxidation of toluene in the presence of NO_x and 1-propene, *Environ. Sci. Technol.*, 35, 3626–3639, 2001.
- Jang, M., Czoschke, N. M., Lee, S., and Kamens, R. M.: Heterogeneous atmospheric aerosol production by acid-catalyzed particle-phase reactions, *Science*, 298, 814–817, 2002.
- Jimenez, J. L., Canagaratna, M. R., Donahue, N. M., Prevot, A. S. H., Zhang, Q., Kroll, J. H., DeCarlo, P. F., Allan, J. D., Coe, H., Ng, N. L., Aiken, A. C., Docherty, K. S., Ulbrich, I. M.,

- Grieshop, A. P., Robinson, A. L., Duplissy, J., Smith, J. D., Wilson, K. R., Lanz, V. A., Hueglin, C., Sun, Y. L., Tian, J., Laaksonen, A., Raatikainen, T., Rautiainen, J., Vaattovaara, P., Ehn, M., Kulmala, M., Tomlinson, J. M., Collins, D. R., Cubison, M. J., Dunlea, E. J., Huffman, J. A., Onasch, T. B., Alfarra, M. R., Williams, P. I., Bower, K., Kondo, Y., Schneider, J., Drewnick, F., Borrmann, S., Weimer, S., Demerjian, K., Salcedo, D., Cottrell, L., Griffin, R., Takami, A., Miyoshi, T., Hatakeyama, S., Shimono, A., Sun, J. Y., Zhang, Y. M., Dzepina, K., Kimmenl, R., Sueper, D., Jayne, J. T., Herndon, S. C., Trimborn, A. M., Williams, L. R., Wood, E. C., Middlebrook, A. M., Kolb, C. E., Baltensperger, U., and Worsnop, D. R.: Evolution of organic aerosols in the atmosphere, *Science*, 326, 1525–1529, 2009.
- Johnson, D., Jenkin, M. E., Wirtz, K., and Martin-Reviejo, M.: Simulating the formation of secondary organic aerosol from the photooxidation of toluene, *Environ. Chem.*, 1, 150–165, 2004.
- Johnson, D., Jenkin, M. E., Wirtz, K., and Martin-Reviejo, M.: Simulating the formation of secondary organic aerosol from the photooxidation of aromatic hydrocarbons, *Environ. Chem.*, 2, 35–48, 2005.
- Kalberer, M., Paulsen, D., Sax, M., Steinbacher, M., Dommen, J., Prevot, A. S. H., Fisseha, R., Weingartner, E., Frankevich, V., Zenobi, R., and Baltensperger, U.: Identification of polymers as major components of atmospheric organic aerosols, *Science*, 303, 1659–1662, 2004.
- Kelly, J. L., Michelangeli, D. V., Makar, P. A., Hastie, D. R., Mozurkewich, M., and Auld, J.: Aerosol speciation and mass prediction from toluene oxidation under high NO_x conditions, *Atmos. Environ.*, 44, 361–369, 2010.
- Kleindienst, T. E., Smith, D. F., Li, W., Edney, E. O., Driscoll, D. J., Speer, R. E., Weathers, W. S.: Secondary organic aerosol formation from the oxidation of aromatic hydrocarbons in the presence of dry submicron ammonium sulfate aerosol, *Atmos. Environ.*, 33, 3669–3681, 1999.
- Kroll, J. H. and Seinfeld, J. H.: Chemistry of secondary organic aerosol: Formation and evolution of low-volatility organics in the atmosphere, *Atmos. Environ.*, 42, 3593–3624, 2008.
- Kroll, J. H., Donahue, N. M., Jimenez, J. L., Kessler, S. H., Canagaratna, M. R., Wilson, K. R., Altieri, K. E., Mazzoleni, L. R., Wozniak, A. S., Bluhm, H., Mysak, E. R., Smith, J. D., Kolb, C. E., and Worsnop, D. R.: Carbon oxidation state as a metric for describing the chemistry of atmospheric organic aerosol, *Nature Chemistry*, 3, 133–139, 2011.
- Lambe, A. T., Onasch, T. B., Massoli, P., Croasdale, D. R., Wright, J. P., Ahern, A. T., Williams, L. R., Worsnop, D. R., Brune, W. H., and Davidovits, P.: Laboratory studies of the chemical composition and cloud condensation nuclei (CCN) activity of secondary organic aerosol (SOA) and oxidized primary organic aerosol (OPOA), *Atmos. Chem. Phys.*, 11, 8913–8928, doi:10.5194/acp-11-8913-2011, 2011.
- Lane, T. E., Donahue, N. M., and Pandis, S. N.: Simulating secondary organic aerosol formation using the volatility basis-set approach in a chemical transport model, *Atmos. Environ.*, 42, 7439–7451, 2008.
- Li, C.-M., Taneda, S., Suzuki, A., Furuta, C., Watanabe, G., and Taya, K.: Anti-androgenic activity of 3-methyl-4-nitrophenol in diesel exhaust particles, *Eur. J. Pharmacol.*, 543, 194–199, 2006.
- Lim, H. J., Carlton, A. G., and Turpin, B. J.: Isoprene forms secondary organic aerosol through cloud processing: Model simulations, *Environ. Sci. Technol.*, 39, 4441–4446, 2005.
- Loza, C. L., Chhabra, P. S., Yee, L. D., Craven, J. S., Flagan, R. C., and Seinfeld, J. H.: Chemical aging of *m*-xylene secondary organic aerosol: laboratory chamber study, *Atmos. Chem. Phys.*, 12, 151–167, doi:10.5194/acp-12-151-2012, 2012.
- Lun, X., Takami, A., Miyoshi, T., and Hatakeyama, S.: Characteristic of organic aerosol in a remote area of Okinawa Island, *J. Environ. Sci.*, 21, 1371–1377, 2009.
- Martin-Reviejo, M. and Wirtz, K.: Is benzene a precursor for secondary organic aerosol?, *Environ. Sci. Technol.*, 39, 1045–1054, 2005.
- Myriokefalitakis, S., Tsigaridis, K., Mihalopoulos, N., Sciare, J., Nenes, A., Kawamura, K., Segers, A., and Kanakidou, M.: In-cloud oxalate formation in the global troposphere: a 3-D modeling study, *Atmos. Chem. Phys.*, 11, 5761–5782, doi:10.5194/acp-11-5761-2011, 2011.
- Nakao, S., Clark, C., Tang, P., Sato, K., and Cocker III, D.: Secondary organic aerosol formation from phenolic compounds in the absence of NO_x, *Atmos. Chem. Phys.*, 11, 10649–10660, doi:10.5194/acp-11-10649-2011, 2011.
- Nakayama, T., Matsumi, Y., Sato, K., Imamura, T., Yamazaki, A., and Uchiyama, A.: Laboratory studies on optical properties of secondary organic aerosols generated during the photooxidation of toluene and the ozonolysis of α -pinene, *J. Geophys. Res.*, 115, D24204, doi:10.1029/2010JD014387, 2010.
- Nakayama, T., Sato, K., Matsumi, Y., Imamura, T., Yamazaki, A., and Uchiyama, A.: Wavelength and NO_x dependent complex refractive index of SOAs generated from the photooxidation of toluene, *Atmos. Chem. Phys. Discuss.*, accepted, 2012.
- Ng, N. L., Kroll, J. H., Chan, A. W. H., Chhabra, P. S., Flagan, R. C., and Seinfeld, J. H.: Secondary organic aerosol formation from *m*-xylene, toluene, and benzene, *Atmos. Chem. Phys.*, 7, 3909–3922, doi:10.5194/acp-7-3909-2007, 2007.
- Ng, N. L., Canagaratna, M. R., Zhang, Q., Jimenez, J. L., Tian, J., Ulbrich, I. M., Kroll, J. H., Docherty, K. S., Chhabra, P. S., Bahreini, R., Murphy, S. M., Seinfeld, J. H., Hildebrandt, L., Donahue, N. M., DeCarlo, P. F., Lanz, V. A., Prévôt, A. S. H., Dinar, E., Rudich, Y., and Worsnop, D. R.: Organic aerosol components observed in Northern Hemispheric datasets from Aerosol Mass Spectrometry, *Atmos. Chem. Phys.*, 10, 4625–4641, doi:10.5194/acp-10-4625-2010, 2010.
- Ng, N. L., Canagaratna, M. R., Jimenez, J. L., Chhabra, P. S., Seinfeld, J. H., and Worsnop, D. R.: Changes in organic aerosol composition with aging inferred from aerosol mass spectra, *Atmos. Chem. Phys.*, 11, 6465–6474, doi:10.5194/acp-11-6465-2011, 2011.
- Noda, J., Volukamer, R., and Molina, M. J.: Dealkylation of alkylbenzenes: A significant pathway in the toluene, *o*-, *m*-, *p*-xylene + OH reaction, *J. Phys. Chem. A*, 113, 9658–9666, 2009.
- Odum, J. R., Jungkamp, T. P. W., Griffin, R. J., Forstner, H. J. L., Flagan, R. C., and Seinfeld, J. H.: Aromatics, reformulated gasoline, and atmospheric organic aerosol formation, *Environ. Sci. Technol.*, 31, 1890–1897, 1997.
- Qi, L., Nakao, S., Malloy, Q., Warren, B., and Cocker III, D. R.: Can secondary organic aerosol formed in an atmospheric simulation chamber continuously age?, *Atmos. Environ.*, 44, 2990–2995, 2010.
- Sato, K.: Detection of nitrooxypolyols in secondary organic aerosol formed from the photooxidation of conjugated dienes under

- high-NO_x conditions, *Atmos. Environ.*, 42, 6851–6861, 2008.
- Sato, K., Klotz, B., Hatakeyama, S., Imamura, T., Washizu, Y., Matsumi, Y., and Washida, N.: Secondary organic aerosol formation during the photo-oxidation of toluene: Dependence on initial hydrocarbon concentration, *Bull. Chem. Soc. Jpn.*, 77, 667–671, 2004.
- Sato, K., Hatakeyama, S., and Imamura, T.: Secondary organic aerosol formation during the photooxidation of toluene: NO_x dependence of chemical composition, *J. Phys. Chem. A*, 111, 9796–9808, 2007.
- Sato, K., Takami, A., Isozaki, T., Hikida, T., Shimono, A., and Imamura, T.: Mass spectrometric study of secondary organic aerosol formed from the photo-oxidation of aromatic hydrocarbons, *Atmos. Environ.*, 44, 1080–1087, 2010.
- Sato, K., Nakao, S., Clark, C. H., Qi, L., and Cocker III, D. R.: Secondary organic aerosol formation from the photooxidation of isoprene, 1,3-butadiene, and 2,3-dimethyl-1,3-butadiene under high NO_x conditions, *Atmos. Chem. Phys.*, 11, 7301–7317, doi:10.5194/acp-11-7301-2011, 2011.
- Shilling, J. E., Chen, Q., King, S. M., Rosenoern, T., Kroll, J. H., Worsnop, D. R., DeCarlo, P. F., Aiken, A. C., Sueper, D., Jimenez, J. L., and Martin, S. T.: Loading-dependent elemental composition of α -pinene SOA particles, *Atmos. Chem. Phys.*, 9, 771–782, doi:10.5194/acp-9-771-2009, 2009.
- Shiraiwa, M., Ammann, M., Koop, T., and Pöschl, U.: Gas uptake and chemical aging of semisolid organic aerosol particles, *P. Natl. Acad. Sci. USA*, 108, 11003–11008, 2011.
- Song, C., Na, K., and Cocker III, D. R.: Impact of the hydrocarbons to NO_x ratio on secondary organic aerosol formation, *Environ. Sci. Technol.*, 39, 3143–3149, 2005.
- Stroud, C. A., Makar, P. A., Michelangeli, D. V., Mozurkewich, M., Hastie, D. R., Barbu, A., and Humble, J.: Simulating organic aerosol formation during the photooxidation of toluene/NO_x mixtures: comparing the equilibrium and kinetic assumption, *Environ. Sci. Technol.*, 38, 1471–1479, 2004.
- Surratt, J. D., Murphy, S. M., Kroll, J. H., Ng, N. L., Hildebrandt, L., Sorooshian, A., Szmigielski, R., Vermeylen, R., Mauenhaut, W., Claeys, M., Flagan, R. C., and Seinfeld, J. H.: Chemical composition of secondary organic aerosol formation from the photooxidation of isoprene, *J. Phys. Chem. A*, 110, 9665–9690, 2006.
- Surratt, J. D., Chan, A. W. H., Eddingsaas, N. C., Chan, M. N., Loza, C. L., Kwan, A. J., Hersey, S. P., Flagan, R. C., Wennberg, P. O., and Seinfeld, J. H.: Reactive intermediates revealed in secondary organic aerosol formation from isoprene, *P. Natl. Acad. Sci. USA*, 1007, 6640–6645, 2010.
- Takami, A., Miyoshi, T., Shimono, A., Kaneyasu, N., Kato, S., Kajii, Y., and Hatakeyama, S.: Transport of antropogenic aerosols from Asia and subsequent chemical transformation, *J. Geophys. Res.*, 112, D22S31, doi:10.1029/2006JD008120, 2007.
- Takegawa, N., Miyakawa, T., Watanabe, M., Kondo, Y., Miyazaki, Y., Han, S., Zhao, Y., van Pinxteren, D., Brüggemann, E., Gnauk, T., Herrmann, H., Xiao, R., Deng, Z., Hu, M., Zhu, T., and Zhang, Y.: Performance of an Aerodyne Aerosol Mass Spectrometer (AMS) during intensive campaigns in China in the summer of 2006, *Aerosol Sci. Tech.*, 43, 189–204, 2009.
- Takekawa, H., Minoura, H., and Yamazaki, S.: Temperature dependence of secondary organic aerosol formation by photo-oxidation of hydrocarbons, *Atmos. Environ.*, 37, 3413–3424, 2003.
- Virtanen, A., Joutsensaari, J., Koop, T., Kannosto, J., Yli-Pirilä, P., Leskinen, J., Mäkelä, J. M., Holopainen, J. K., Pöschl, U., Kulmala, M., Worsnop, D. R., and Laaksonen, A.: An amorphous solid state of biogenic secondary organic aerosol particles, *Nature*, 467, 824–825, 2010.
- Wang, Y., Kim, H., and Paulson, S. E.: Hydrogen peroxide generation from α - and β -pinene and toluene secondary organic aerosols, *Atmos. Environ.*, 45, 3149–3156, 2011.
- Wang, Y., Arellanes, C., and Paulson, S. E.: Hydrogen peroxide associated with ambient fine-mode, diesel, and biodiesel aerosol particles in Southern California, *Aerosol Sci. Tech.*, 46, 394–402, 2012.
- Zhang, Q., Jimenez, J. L., Canagaratna, M. R., Allan, J. D., Coe, H., Ulbrich, I., Alfarra, M. R., Takami, A., Middlebrook, A. M., Sun, Y. L., Dzepina, K., Dunlea, E., Docherty, K., DeCarlo, P. F., Salcedo, D., Onasch, T., Jayne, J. T., Miyoshi, T., Shimono, A., Hatakeyama, S., Takegawa, N., Kondo, Y., Schneider, J., Drewnick, F., Borrmann, S., Weimer, S., Demerjian, K., Williams, P., Bower, K., Bahreini, R., Cottrell, L., Griffin, R. J., Rautiainen, J., Sun, J. Y., Zhang, Y. M., and D. R. Worsnop: Ubiquity and dominance of oxygenated species in organic aerosols in anthropogenically-influenced Northern Hemisphere midlatitudes, *Geophys. Res. Lett.*, 34, L13801, doi:10.1029/2007GL029979, 2007.
- Zhang, X., Lin, Y.-H., Surratt, J. D., Zotter, P., Prévôt, A. S. H., and Weber, R. J.: Light-absorbing soluble organic aerosol in Los Angeles and Atlanta: A contrast in secondary organic aerosol, *Geophys. Res. Lett.*, 38, L21810, doi:10.1029/2011GL049385, 2011.